

(NASA-CR-132556) POWER REQUIREMENT OF
ROTATING RODS IN AIRFLOW (Old Dominion Univ.
Research Foundation) 19 p HC \$3.25 CSCL 01B

N75-14716

Unclas

G3/02 07573

POWER REQUIREMENT OF ROTATING RODS IN AIRFLOW

A TECHNICAL REPORT

By

P. S. Barna

and

Gary R. Crossman

Prepared for the
NATIONAL AERONAUTICS AND SPACE ADMINISTRATION
Langley Research Center
Hampton, Virginia 23665

Under
Master Contract Agreement NAS1-11707
Task Authorization No. 60

School of Engineering
Old Dominion University
Technical Report 74-M6

Submitted by the
Old Dominion University Research Foundation
P. O. Box 6173
Norfolk, Virginia 23508

September 1974



POWER REQUIREMENT OF ROTATING RODS IN AIRFLOW

by

P. S. Barna¹

and

Gary R. Crossman²

ABSTRACT

Experiments were performed to determine the power required for rotating a rotor disc fitted with a number of radially arranged rods placed into a ducted airflow. An array of stationary rods, also radially arranged, were placed upstream close to the rotor with a small gap between the rods to cause wake interference.

The results show that power increased with increasing airflow and the rate of increase varied considerably. At lower values of airflow the rate of increase was larger than at higher airflow and definite power peaks occurred at certain airflow rates, where the power attained a maximum within the test airflow range. During the test a maximum blade passage frequency of 2037 Hz was attained.

**REPRODUCIBILITY OF THE
ORIGINAL PAGE IS POOR**

POWER REQUIREMENT OF ROTATING RODS IN AIRFLOW

by

P. S. Barna¹

and

Gary R. Crossman²

SUMMARY

Experiments were performed to determine the power required for rotating a rotor disc fitted with a number of radially arranged rods placed into a ducted airflow. An array of stationary rods, also radially arranged, were placed upstream close to the rotor with a small gap between the rods to cause wake interference.

The results show that power increased with increasing airflow and the rate of increase varied considerably. At lower values of airflow the rate of increase was larger than at higher airflow and definite power peaks occurred at certain airflow rates, where the power attained a maximum within the test airflow range. During the test a maximum blade passage frequency of 2037 Hz was attained.

¹ Professor of Mechanical Engineering, School of Engineering, Old Dominion University, Norfolk, Virginia 23508.

² Assistant Professor of Engineering Technology, School of Engineering, Old Dominion University, Norfolk, Virginia 23508.

SYMBOLS

A	area, m^2
C_D	drag coefficient
C_p	power coefficient
D	tip diameter of rotor ($2R_o$)
F	force, Newton
m	number of rods
N	rotational speed, revolutions per minute (rpm)
P	power required to drive rotor, watts
r	radius, m
R_i	hub radius, m
R_o	tip radius, m
t	rod diameter, mm (millimeter)
T	torque, Newton-meter
U	tangential velocity, m/s
V_a	axial velocity in empty annulus, m/s
ω	angular speed, radians per second
ρ	air density, kg/m^3
ν	kinematic viscosity, m^2/s

APPARATUS

The test equipment consisted of a duct system in which a set of rods were rotated downstream in the wake of a set of stationary rods.

The cylindrical duct housing the rods was made of heavy-gage steel through which the air flow was induced by a centrifugal blower driven by a 15 hp variable speed motor. The air entered the duct through a well-rounded inlet, then passed over the stationary rods, subsequently passed over the rotating rods and, after expanding through a diffuser, entered the intake of the blower. From the discharge side of the blower, the air passed over a damper and upon turning a corner it entered a calming chamber and was finally exhausted at the top of the chamber through a suitable orifice plate. The general layout of the apparatus is shown in Fig. 1, while photographic views are shown in Figs. 2 and 3.

A wide range of flow conditions could be obtained by changing the rotational speed of the blower, or by varying the size of the orifice openings and also by adjusting the setting of the damper.

There were 30 stationary and 26 rotating rods radially arranged in the duct. All the rods were made of 3/16 in. (4.76 mm)-diameter high tensile aluminum. The rotating rods were turned from 1/2 in. hexagon stock and were provided with a 1/4 in. screw thread at their ends which fitted into a circular rotor disc keyed to the shaft of the drive motor. Details of a rotating rod are given in Fig. 4a. The rotating rods were positioned immediately behind the stationary rods with a small gap left between the two sets of rods. After fitting the rods into the rotor disc a portion of the disc and of the rods at their root was cut away in a lathe to allow the gap to be further reduced to the desired 2 mm distance (see Fig. 4b.)

The stationary rods were cut from 3/16 in. round stock and extended between the central hub and the external casing. Six of these rods were employed to suspend the center hub by a spider web arrangement, while twenty-four rods remained non-structural.

The drive motor to the rotor disc was cradle mounted coaxially with the ducting and was provided with an infinite speed control between the range of 500 to 5000 rpm. For the measurement of torque, an arm of 0.4 m length was mounted to the drive-motor housing which extended through the duct wall. Suitable weights were placed on the arm to provide the necessary torque balance. The arm with the sliding weight in zero position was balanced in a horizontal position by a spring of which the tension could be adjusted. A scale, mounted parallel with the torque arm, facilitated the reading of the weight displacement.

In order to estimate in advance the approximate size of the motor needed for the experiments it was necessary to determine the torque for rotating the rods. Since the torque from the motor was required to overcome the drag produced by the rods, it was assumed that they were moving in stationary air. It was further assumed that tip and hub effects were negligible and that no interference between stationary and rotating rods existed. Details of this approximate calculation are given in Appendix A.

The centrifugal blower was equipped with a four-speed control permitting 1760, 1175, 875, and 575 rpm to be maintained. The orifice plate sizes ranged from 0.1 m to 0.4 m in diameter.

For the measurement of air flow, a standard pitot-static tube was installed near the plane of the duct inlet with a single tube inclined manometer used to measure the pressure differential. A standard strobotorch was employed to measure the rotational speed of the rotor.

TEST PROCEDURE

The tests consisted of measuring both the power required for rotating the rods and the noise emitted by them.*

Since both the rotational speed and the air flow rate in the duct could be varied, it was decided to divide the experiments into test runs where each run consisted of keeping the rotational speed of the rotor constant while gradually varying the flow rate from zero to maximum. Accordingly, test runs were made at selected speeds, namely at 2, 3, 4, and 4.7 thousand rpm.

Prior to testing the rotor under operational conditions, a simple method for air flow rate measurement was established to eliminate the laborious recording of a multitude of velocity profiles. A number of velocity profiles were taken over a wide range of flow conditions and these were integrated to furnish the mean air velocity [1]. It was found that the pitot tube could be placed into the air stream at a certain radial location where the mean air velocity intersected the velocity profile, and this location remained almost constant over the entire air flow range. (A small variation of only 1.5 mm was found, which was considered negligible). Ultimately, the point of the pitot tube for measuring the mean air velocity was located at 80-mm distance from the center line.

The size of the counterweight to be used on the balance arm for measuring torque was also established prior to testing. The maximum weight was determined so as to just reach the rated (max) power of the motor (0.75 hp) at maximum speed (5000 rpm) when the weight was placed at the far end of the balance arm. This weight was eventually divided into three parts and one or two parts only were employed for the lower torque readings. This procedure allowed for higher

* Noise measurements were performed by NASA personnel.

accuracy of readings. To facilitate the rotational speed determination with the strobotorch, all but one of the rotating rods were painted with a purple dye. The variable frequency strobe light source was set up about 1 m from the duct inlet in alignment with its centerline and was intermittently operated.

Before each test run, the weights on the torque arm were "zeroed" with the spring tension adjusted to bring the torque arm to a horizontal position. This was repeated whenever a weight was added or removed. A test run generally consisted of the following steps:

- (1) The pitot tube manometer was zeroed, the blower was started, and the airflow was adjusted using the damper and/or orifices to obtain the desired airspeed.
- (2) The rotor was then started and by use of the rheostat the speed was brought to 2000 rpm, this being the minimum speed.
- (3) The air speed and rotor speed were adjusted alternately, since one affected the other, until desired values were obtained.
- (4) The weights were moved along the arm until it assumed horizontal position and balanced the torque.
- (5) The weight displacement, rotor speed, and manometer reading were recorded and the ambient air conditions were noted.

Steps (1) through (5) were then repeated over the range of airspeeds for 2000 rpm, and subsequently repeated for the entire range of selected rotational speeds.

RESULTS AND DISCUSSIONS

Results of the tests are presented in Figs. 5 and 6. In Fig. 5 the power required to drive the rotor is plotted against air velocity for four constant rotor speeds, while in Fig. 6 the same results are "normalized" in a

nondimensional representation. Accordingly, in Fig. 5 the four power curves are plotted against the air velocity in the "empty" annular duct section just upstream from the rods. Thus the passage restriction due to the presence of the rods was not considered.

The normalized power coefficient (C_p) in Fig. 6 is plotted against advance ratio (J) in exactly the same way as propeller coefficients are usually presented [2], namely

$$C_p = \frac{P}{\rho N^3 D^5}$$

$$J = \frac{V_a}{ND}$$

With numerical values $\rho = 1.227 \text{ kg/m}^3$, $D = 0.254 \text{ m}$ the power coefficient becomes

$$C_p = 0.1677 \frac{P(\text{Watts})}{(N/1000)^3}$$

and the advanced ratio

$$J = 0.2362 \frac{V_a}{(N/1000)}$$

All dimensional power curves plotted in Fig. 5 show first a sharp increase with air speed, which is followed by a decrease in gradient before the markedly steep rise leading to a "hump" occurs. After the hump, a sudden decrease in power is experienced with a subsequent levelling off, resulting in a "hollow" or "trough" in the curve. With further increasing air velocity, power again appears to gradually and continuously rise. Both the magnitude of the peaks and their location depends on air velocity and on rotational speed, and a shift to the right is experienced in the peaks with increasing speed.

The normalized or non-dimensional plotting of the results in Fig. 6 shows all observations collapsed on a single curve with highly satisfactory consistency. This remarkable but not altogether unexpected result proves that the rotor may

indeed be considered a special type of propeller which follows the rules of rotodynamic machinery.

The normalized plot more or less follows the general characteristics of the dimensional curves, that is, a steep gradient ahead of the hump, followed by a gradual rise of the power coefficient with further increasing advance ratio. There is, however, the added appearance of two humps and two hollows after the first peak, located at $J = 1.56$ approximately. The second hump peaks at about $J = 3.15$, while the third, less distinct from the first two humps, peaks at $J = 4.6$ approximately. Thus the peaks are located at equal intervals and at a multiple of the advance ratio of the first peak.

The first peak is the most critical as it produces the largest power coefficient, $C_p = 1.32$ approximately. This peak also displays the steepest gradients on either side of the maxima, and at this point, under actual operational conditions the power increased to an estimated 817 watts at 4700 rpm and thus markedly exceeded the available motor capacity. This power peak prevented fully attaining the 5000 rpm design speed and the 2500 Hz design passage frequency which was based on the number of rotor rods.

The probable source of the peaks may be attributed to wake interference between the rotating and stationary rods where vibration of the rotating rods is probably set up by the vortex shedding of the stationary rods. The possibility of critical Reynolds number as a cause of this effect must be discounted. The maximum rod Reynolds number, based on rod diameter t and absolute velocity* as well as its largest peak value, occurs at an estimated 1/10th of the critical Reynolds number of a cylinder which is known to be about 2×10^5 [3].

* Absolute velocity = $\sqrt{U^2 + V_a^2}$.

Since the natural frequency [4] of the rotor rods was estimated to be 1469 cps, resonant vibration due to wake effects is unlikely to be the cause of the power peaks.

It is curious that the power peaks become less pronounced at high air velocities. On the assumption that no further peaks occur at velocities in excess of 50 m/s, the power coefficient may attain a value of 1.8 to 2.0 when $V_a = 200$ m/s ($J = 10.1$). Thus at this air velocity, discounting compressibility effects, the power required to drive the rotor would be roughly 2 hp.

CONCLUSION

The objectives of the tests were nearly realized and air flow velocities up to 50 m/s were attained for four rotational speeds of the rotor producing noise frequencies near the desired range. The measured power plotted against air speed produced curves that show three power peaks of which the first and by far the largest did not occur at the maximum air speed as anticipated but at a much lower value. This peak occurred at a Reynolds number of one order of magnitude less than the established critical Reynolds number for flow over cylinders. Further studies are required to explore the nature of these peaks and to find a plausible explanation.

REFERENCES

1. A.S.M.E. Fluid Meters, their theory and application.
also
Barna, P. S.: Fluid Mechanics for Engineers, Butterworth, 3rd Ed. 1969,
p. 120.
2. Millikan, Clark B.: Aerodynamics of the Airplane, Wiley & Sons, 1971,
p. 116-117.
3. Goldstein, S. (Editor): Modern developments in Fluid Dynamics, Oxford
Press, 1938, Vol. II, p. 419.
4. Den Hartog, J. P.: Mechanical Vibrations, 4th Ed., McGraw Hill, 1962,
p. 432.

Appendix A

Consider a cylindrical element of a single rod with a projected area, $dA = t dr$. The torque required to overcome the drag of that element is given by $dT = r dF_D$. The drag force may be represented by $dF_D = 1/2 \rho C_D U^2 dA$. Since the tangential velocity of the element $U = r\omega$, $dT = r dF_D = r \cdot 1/2 \rho C_D (r\omega)^2 t dr = 1/2 \rho C_D \omega^2 t r^3 dr$. For incompressible flow ρ can be considered constant, however C_D may vary with the Reynolds number based on tangential speed and rod diameter $N_R = Ut/\nu = r\omega t/\nu$. A range of Reynolds number can be calculated using the lowest and highest angular velocity anticipated during testing at the hub and the tip radius respectively.

With the Reynolds numbers calculated C_D varies from 0.95 to 1.05 (see Ref. 3), thus a constant mean value of 1.0 seemed a reasonable assumption.

Assuming $C_D = \bar{C}_D$, upon integration, torque for a single rod becomes

$$T = 1/2 \rho C_D \omega^2 t \int_{R_i}^{R_o} r^3 dr = 1/8 \rho C_D \omega^2 t (R_o^4 - R_i^4)$$

For m number of rods T must be multiplied by m . With the numerical values $\rho = 1.227 \text{ kg/m}^3$, $C_D = 1.0$, $m = 26$, $t = 4.76 \text{ mm}$, $R_o = .127 \text{ m}$, $R_i = .07 \text{ m}$ one obtains torque

$$T = .049 \left(\frac{N}{1000} \right)^2$$

Since power $P = T\omega$,

$$P = 5.13 \left(\frac{N}{1000} \right)^3$$

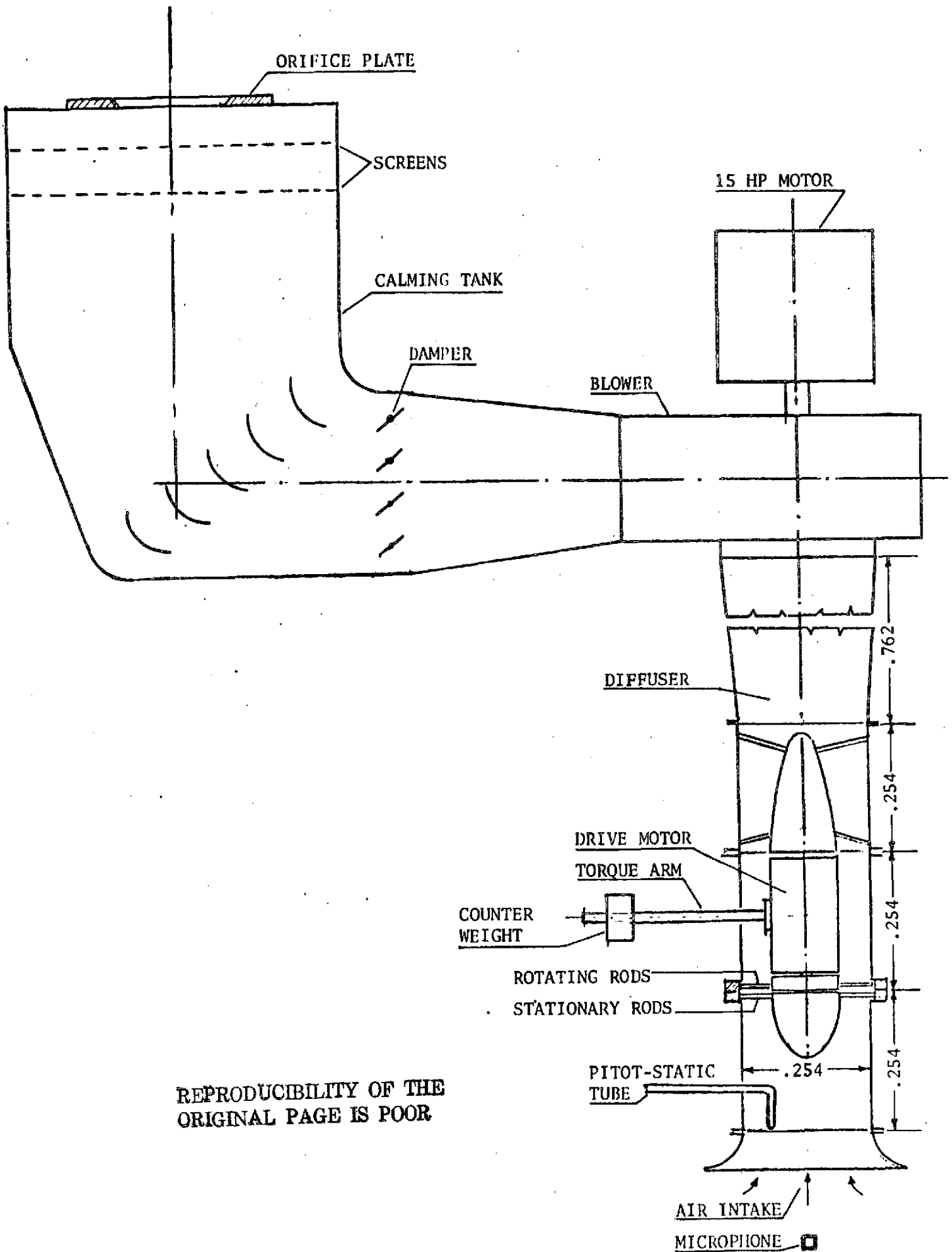
Thus the anticipated maximum speed of 5000 rpm yields

$$T = .049(5)^2 = 1.225 \text{ Nm}$$

and

$$P = (5.13)(5)^3 = 641.25 \text{ watts or } 0.86 \text{ hp,}$$

which is slightly above the rated power of the motor used.



REPRODUCIBILITY OF THE ORIGINAL PAGE IS POOR

Figure 1. General lay-out of test equipment. All dimensions in meters.

REPRODUCIBILITY OF THE
ORIGINAL PAGE IS POOR.

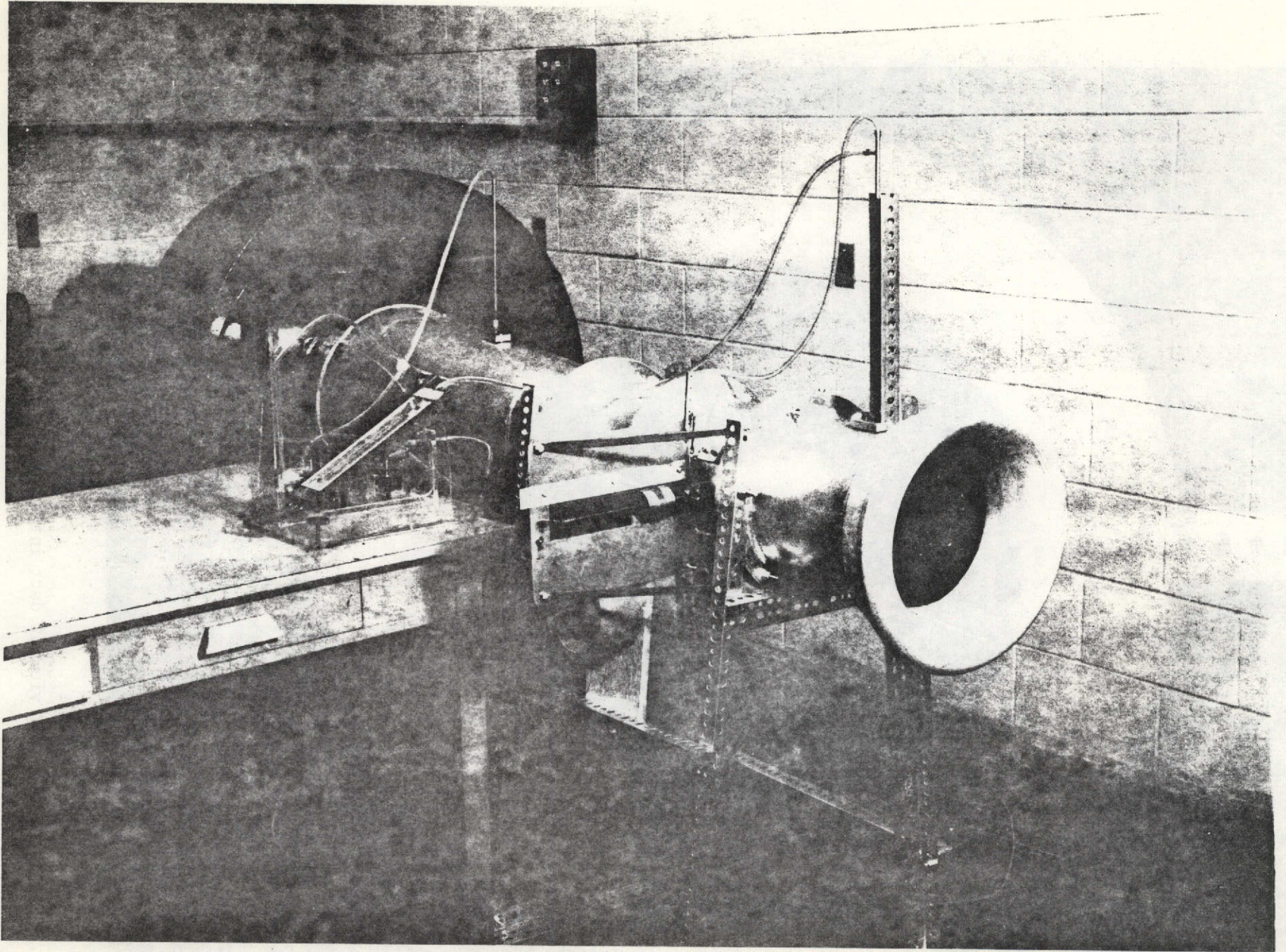


Figure 2. View of experimental set-up.

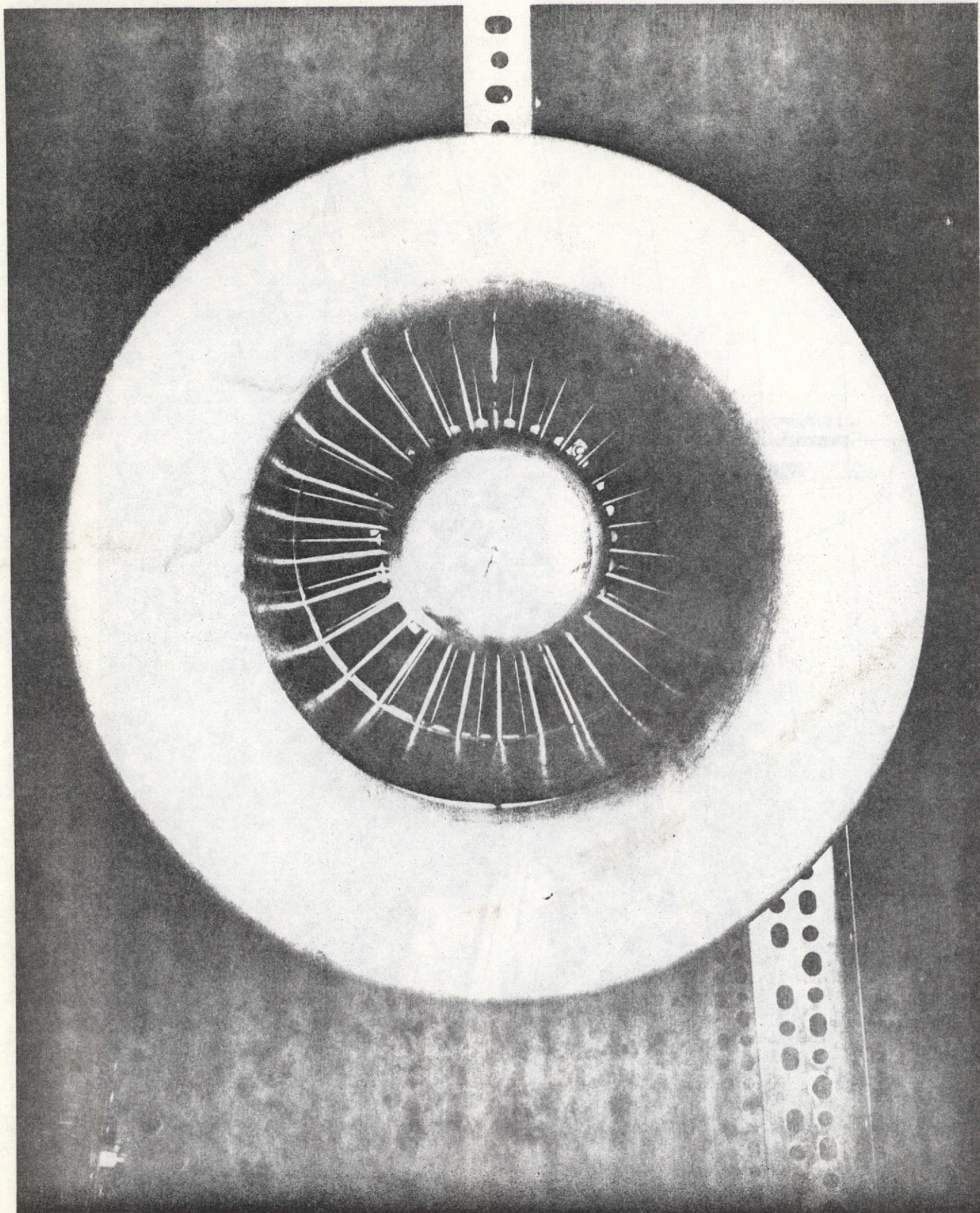


Figure 3. Frontal view of duct intake showing stator and rotor.

REPRODUCIBILITY OF THE
ORIGINAL PAGE IS POOR

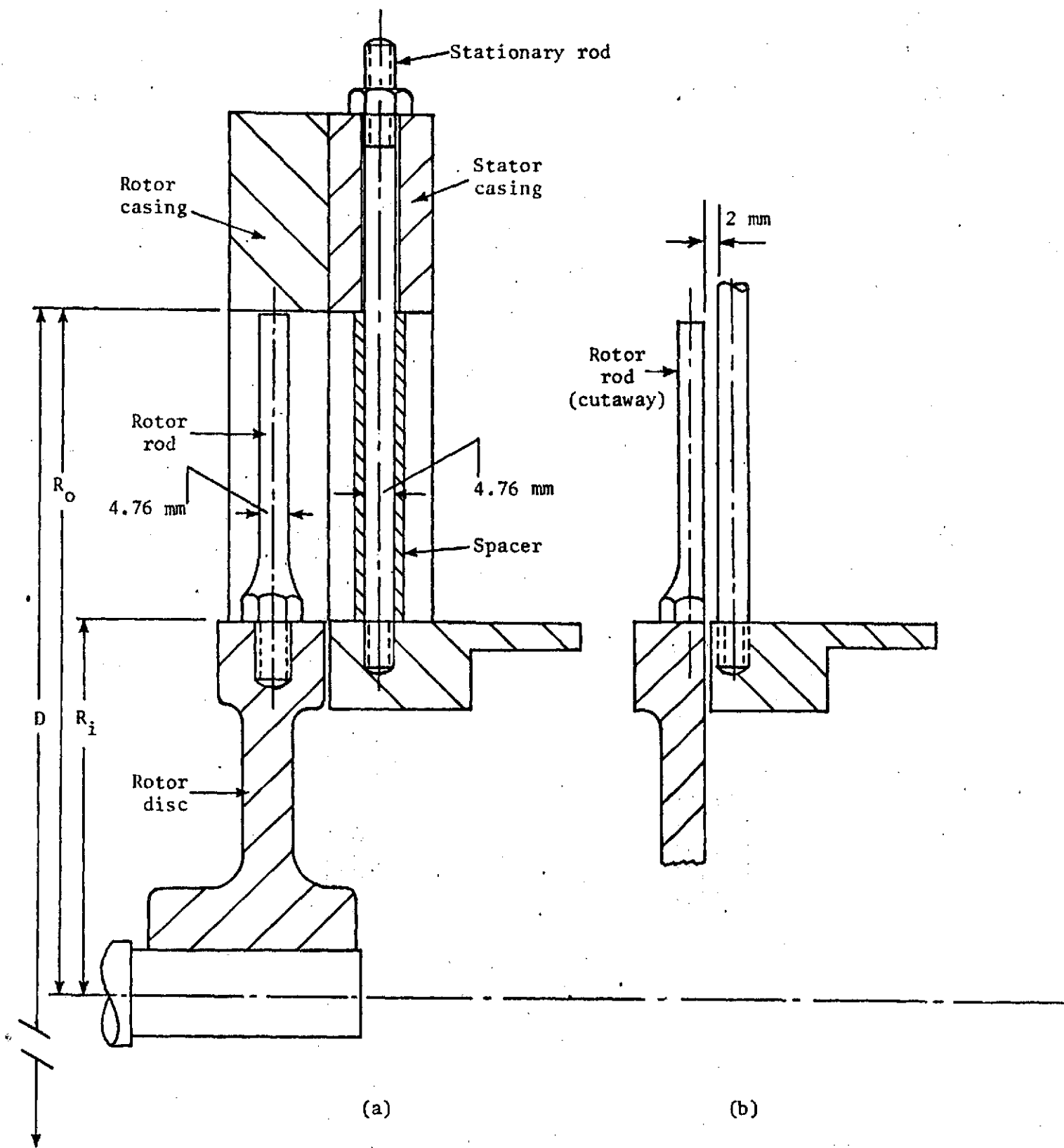


Figure 4. Sectional view of rotor and stator.

REPRODUCIBILITY OF THE ORIGINAL PAGE IS POOR

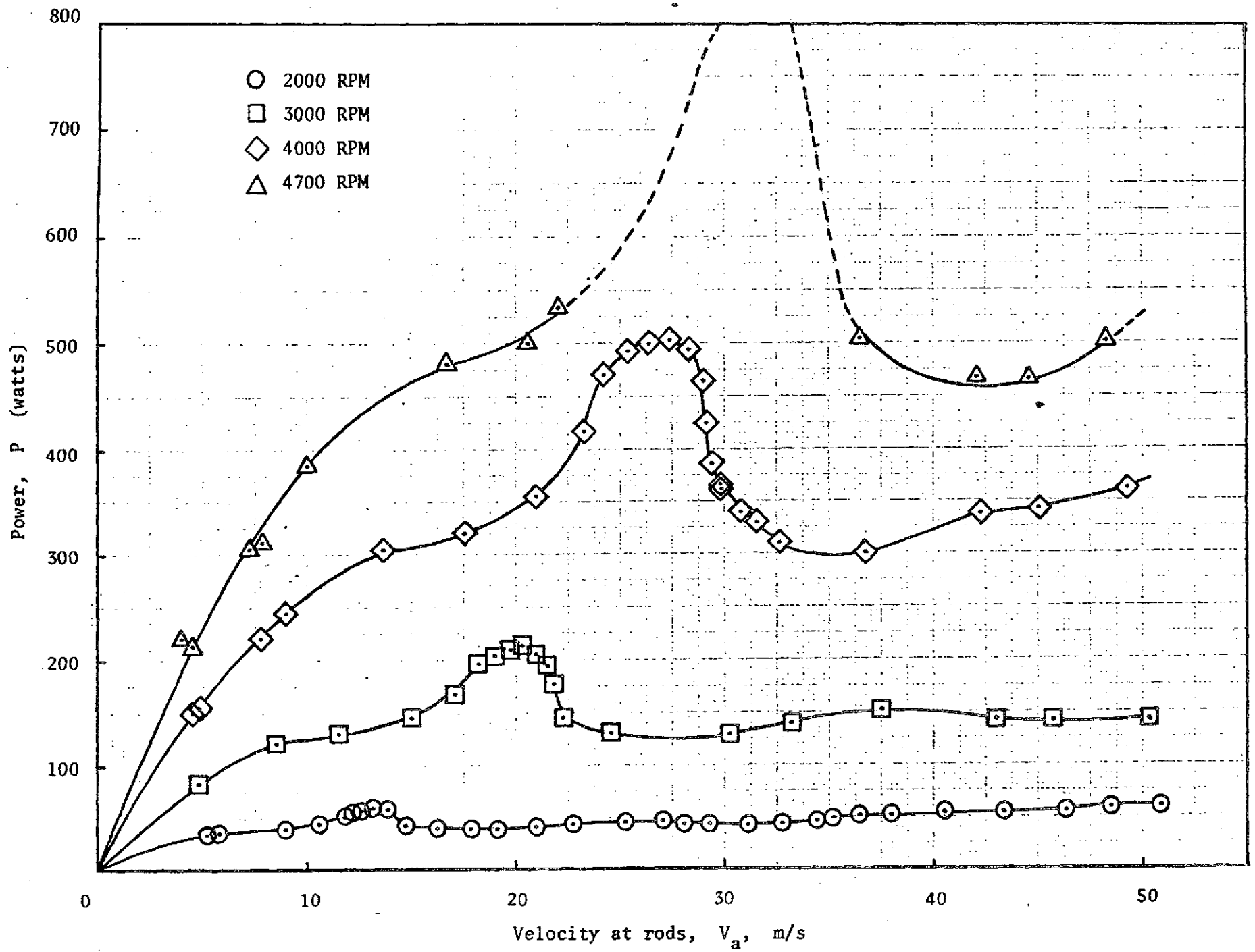


Figure 5. Variation of drive motor power with airspeed.

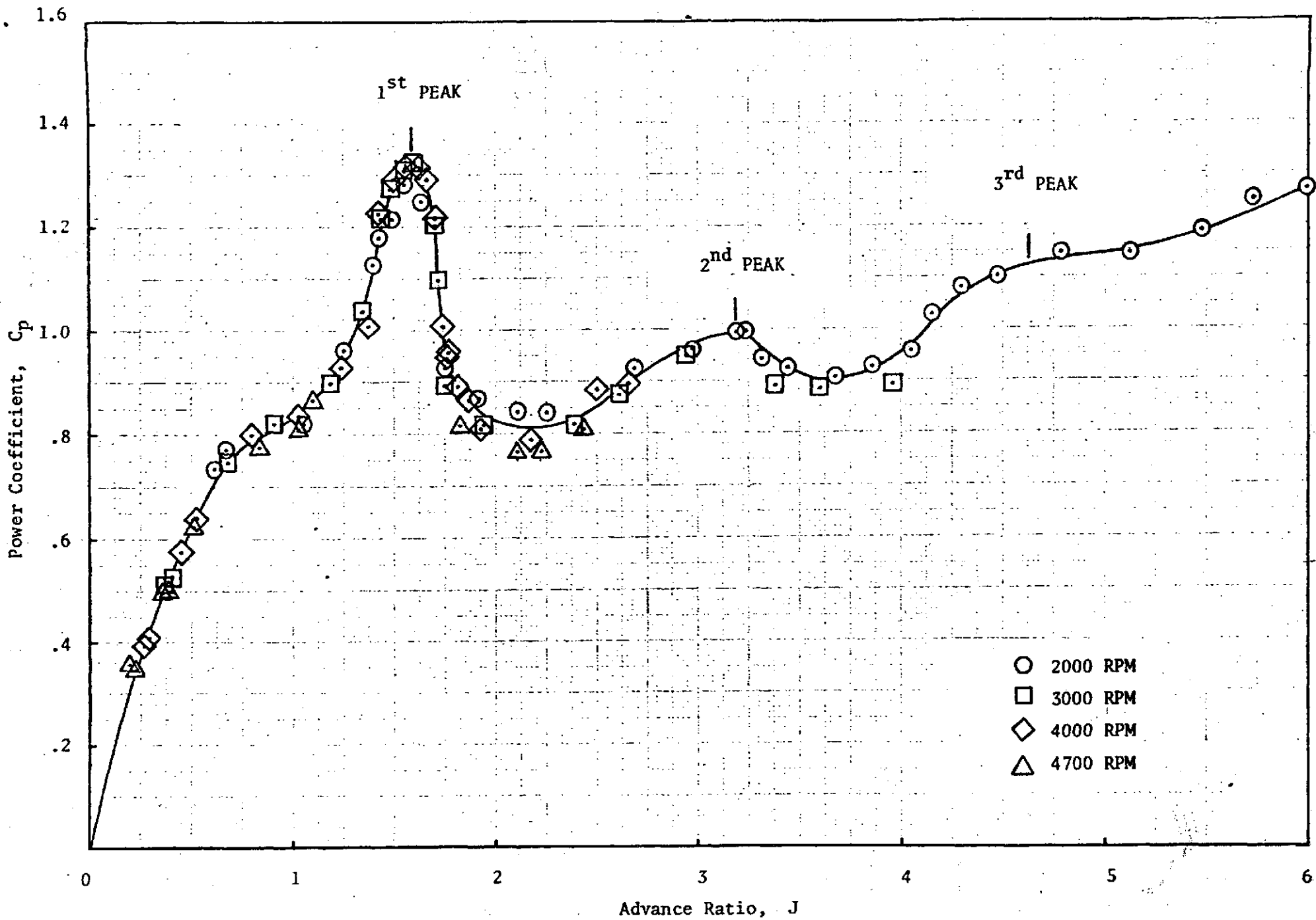


Figure 6. Variation of power coefficient with advance ratio.